Local Phase Velocity Based Imaging (LPVI): A New Technique Used For Ultrasound Shear Wave Elastography - Supplementary Material

Tables S1-S3 present mean, median, standard deviation, variance, maximum and minimum values of shear wave velocity calculated for the liver fibrosis tissue mimicking homogeneous phantoms using the LPVI approach. Results are presented for phantoms with nominal Young's moduli of 10, 25 and 45 kPa, respectively.

Figure S1 shows the bias of the mean phase velocity computed for the homogeneous liver fibrosis tissue mimicking phantoms for various frequencies and the spatial window dimensions for LPVI. Bias was calculated using an expression

$$Bias = \frac{\bar{c}_{ph}^{LPVI} - c_{ph}^{NOM}}{c_{ph}^{NOM}} \cdot 100\% \tag{S1}$$

where $\bar{c}_{ph}^{LPVI}$ is a mean phase velocity within ROI calculated using LPVI. c_{ph}^{NOM} is a true phase velocity computed twofold: (1) using known elasticity and density via an expression $c_{ph}^{NOM} = \sqrt{E/(3\rho)}$ or (2) using a classical two-dimensional Fourier transform (2D-FT) method in order to calculate dispersion curves.

Data in Fig. S1 are presented for the liver fibrosis tissue mimicking homogeneous phantoms for ROIs presented in Fig. 3 in the main manuscript.

Figures S2 and S3 show bias of the mean phase velocity computed for LISA data and CIRS phantom from an inclusion phantom with 6.49 mm diameter for background and inclusion, respectively. ROIs for the background and inclusion are marked in Fig. 2 in the main manuscript. Results are presented for various frequencies and the spatial window dimensions for (a) nominal elasticity provided by manufacturer, and (b) phase velocity calculated using classical 2D-FT method shown in Fig. 8c.

Figure S4 presents two-dimensional shear wave phase velocity images for the CIRS phantom with an inclusion Type IV and size of 10.40 mm (top row), 6.49 mm (middle row) and 4.05 mm (bottom row) of diameter, respectively. Phase velocity images were calculated using LPVI approach. Similar images for inclusions Type III, II and I are presented in Figs. S6, S9 and S11, respectively. Dashed lines present the true inclusion locations estimated from B-modes images. For higher frequencies, starting from approximately 900 Hz, spurious peaks can be observed for inclusions Type I and II which are softer than surrounding background. Softer inclusion suppresses traveling higher frequency components of shear wave before it passes the inclusion through. It is illustrated in Fig. S8 for the inclusion Type II and size of 10.4 mm. The shear wave traveling from the left to the right side of the inclusion (Fig. S8a) could not propagate over that distance. As a result, artifacts in the reconstructed images are present in the bottom right corner. Similar effects are observed when the shear wave travels from the right towards the left side, Fig. S8b. Fig. S8c shows averaged image from maps depicted in Figs. S8a and S8b.

Figure S5 presents two-dimensional shear wave phase velocity images for the CIRS phantom with an inclusion Type IV and size of 10.40 mm (top row), 6.49 mm (middle row) and 4.05 mm (bottom row) of diameter, respectively. Phase velocity images were calculated using phase velocity approach described by Budelli et al. [24]. Similar images for the same method for inclusions Type III, II and I are presented in Figs. S7, S10 and S12, respectively. Dashed lines present true inclusion locations estimated from B-modes images. One can notice that method presented by Budelli et al. is much more influenced by noise. This is visible for all types of inclusion. Moreover, it is even more pronounced for softer inclusions (Type I and II). One of the reasons for that behavior might be that this technique is based on a phase gradient search which is susceptible to changes observed in measured shear wave signal. Secondly, only the lateral direction is taken into account when reconstructing shear wave velocity maps. At the same time LPVI takes into account information from both lateral and axial directions.

Tables S4, S6, S8 and S10 present mean, median, standard deviation, variance, maximum and minimum values of shear wave velocity calculated for the inclusion Type IV, III, II and I, respectively, for the LPVI approach.

Tables S5, S7, S9 and S11 present mean, median, standard deviation, variance, maximum and minimum values of shear wave velocity calculated for the inclusion Type IV, III, II and I, respectively, for phase velocity approach described by Budelli et al. [24].

We used a threshold of 7 m/s when calculating aforementioned values for LPVI and Budelli et al.'s methods in order to bypass spurious phase velocity values higher than 7 m/s.

Figure S13 presents the contrast-to-noise ratio (CNR) estimated fo the LPVI, computed for various frequencies and the spatial window dimensions, calculated for the gelatin phantom experimental data presented in Fig. 16 in the main manuscript.

TABLE S1: Mean, median, standard deviation, variance, maximum and minimum values of shear wave velocity calculated for the liver fibrosis tissue mimicking homogeneous phantom for LPVI approach. Values are presented in the unit of m/s. A nominal Young's modulus provided by the manufacturer is 10 kPa (c = 1.826 m/s). Window size used for LPVI was 3.5 × 3.5 mm.

Young's modulus	**Variable**	**Frequency [Hz]**				
		100	**200**	**300**	**400**	**500**
10 kPa	**MEAN**	1.630	1.640	1.621	1.610	1.610
	MEDIAN	1.606	1.672	1.626	1.601	1.604
	STD	0.086	0.072	0.054	0.034	0.038
	VAR	0.007	0.005	0.003	0.001	0.001
	MAX	1.846	1.820	1.820	1.736	1.731
	MIN	1.455	1.475	1.521	1.524	1.512

TABLE S2: Mean, median, standard deviation, variance, maximum and minimum values of shear wave velocity calculated for the liver fibrosis tissue mimicking homogeneous phantom for LPVI approach. Values are presented in the unit of m/s. A nominal Young's modulus provided by the manufacturer is 25 kPa (c = 2.887 m/s). Window size used for LPVI was 3.5 × 3.5 mm.

Young's modulus	**Variable**	**Frequency [Hz]**					
		100	**200**	**300**	**400**	**500**	**600**
25 kPa	**MEAN**	2.435	2.433	2.428	2.431	2.431	2.432
	MEDIAN	2.421	2.427	2.420	2.425	2.438	2.424
	STD	0.058	0.045	0.052	0.046	0.040	0.047
	VAR	0.003	0.002	0.003	0.002	0.002	0.002
	MAX	2.580	2.569	2.620	2.573	2.572	2.627
	MIN	2.246	2.281	2.291	2.291	2.263	2.281

TABLE S3: Mean, median, standard deviation, variance, maximum and minimum values of shear wave velocity calculated for the liver fibrosis tissue mimicking homogeneous phantom for LPVI approach. Values are presented in the unit of m/s. A nominal Young's modulus provided by the manufacturer is 45 kPa (c = 3.873 m/s). Window size used for LPVI was 3.5 × 3.5 mm.

Young's modulus	**Variable**	**Frequency [Hz]**					
		100	**200**	**300**	**400**	**500**	**600**
45 kPa	**MEAN**	3.496	3.486	3.476	3.466	3.469	3.465
	MEDIAN	3.493	3.504	3.491	3.454	3.471	3.462
	STD	0.111	0.097	0.074	0.071	0.067	0.074
	VAR	0.012	0.009	0.006	0.005	0.005	0.006
	MAX	3.916	3.848	3.669	3.707	3.675	3.705
	MIN	3.142	3.134	3.108	3.230	3.251	3.211

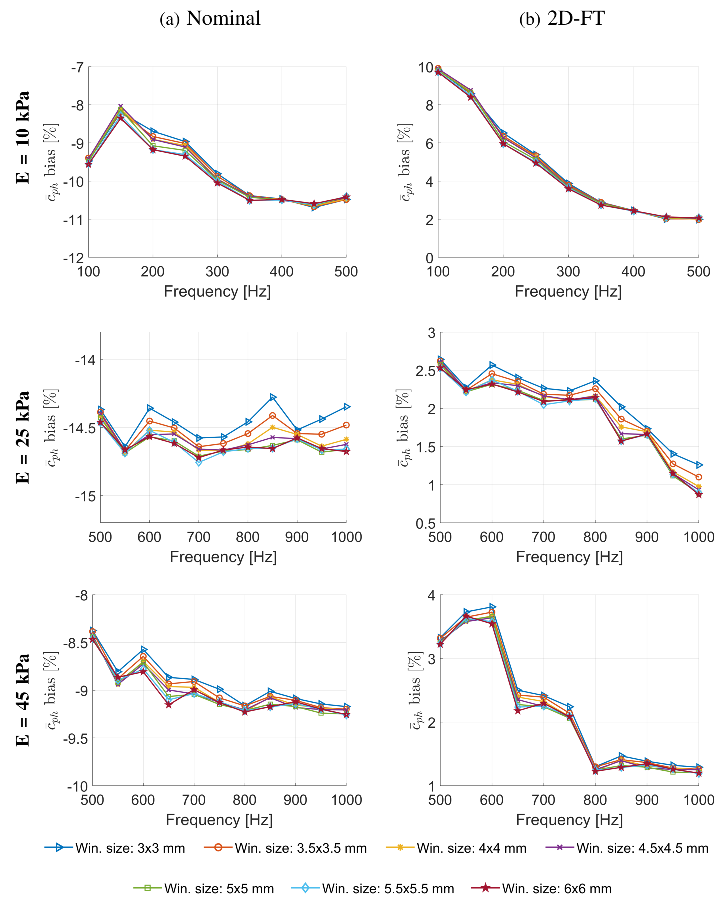

Fig. S1: Bias of the mean phase velocity computed for the homogeneous liver fibrosis tissue mimicking phantoms for various frequencies and the spatial window dimensions for LPVI. Results present bias computed against (a) nominal elasticity provided by manufacturer, and (b) phase velocity calculated using classical 2D-FT method at focused push beam depth. ROIs are presented in Fig. 3 in the main manuscript.

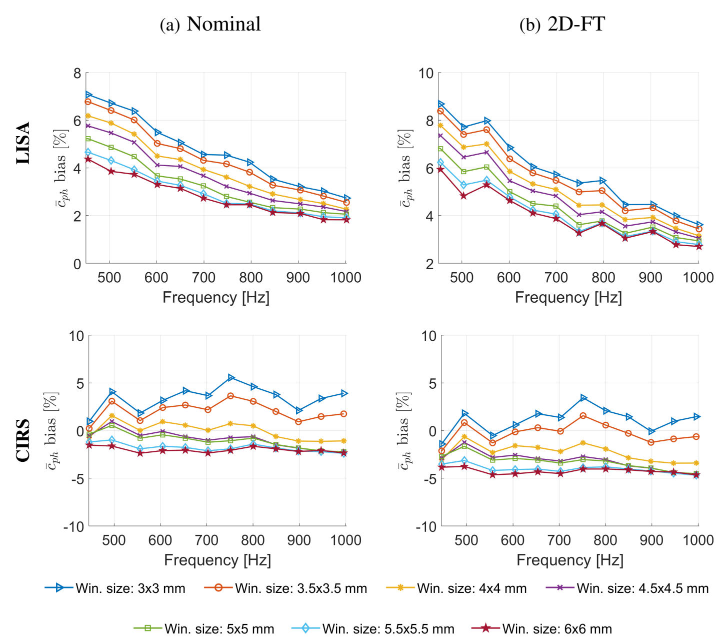

Fig. S2: Bias of the mean phase velocity computed for LISA data and CIRS phantom with stepped cylinders for background. Results are presented for various frequencies and the spatial window dimensions for (a) nominal elasticity provided by manufacturer, and (b) phase velocity calculated using classical 2D-FT method. ROI for the background is marked in Fig. 2 in the main manuscript.

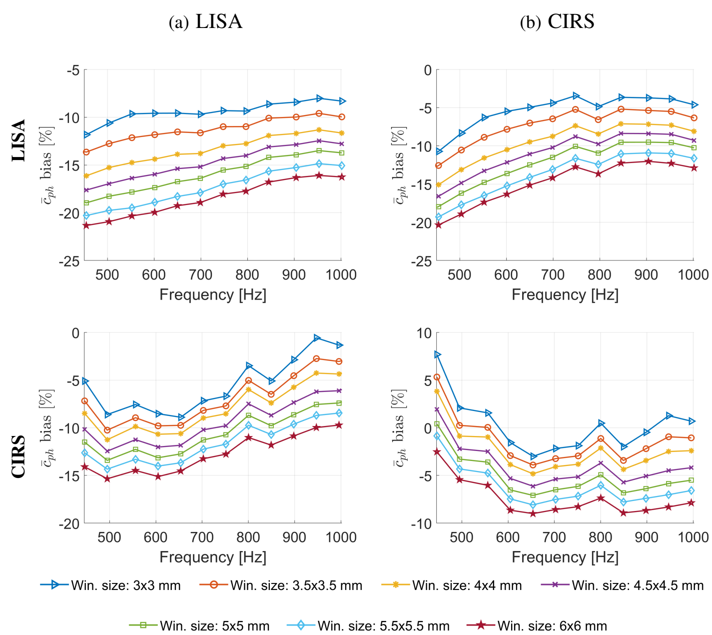

Fig. S3: Bias of the mean phase velocity computed for LISA data and CIRS phantom with stepped cylinders for inclusion. Results are presented for various frequencies and the spatial window dimensions for (a) nominal elasticity provided by manufacturer, and (b) phase velocity calculated using classical 2D-FT method. ROI for the inclusion is marked in Fig. 2 in the main manuscript.

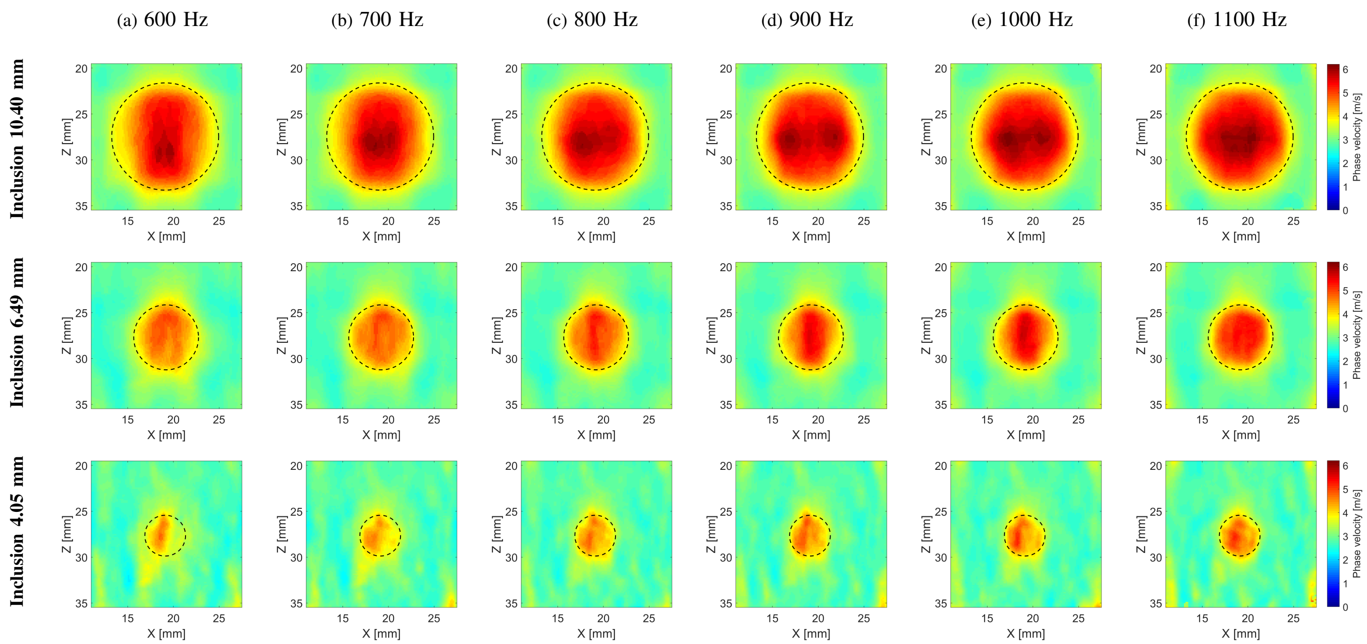

Fig. S4: Two-dimensional shear wave phase velocity images for the inclusion size of 10.40 (top row), 6.49 (middle row) and 4.05 (bottom row) diameter, respectively. Phase velocity images were calculated using LPVI approach. Presented images are computed for the CIRS phantom with an inclusion Type IV. Dashed lines present a true inclusion location estimated from B-modes.

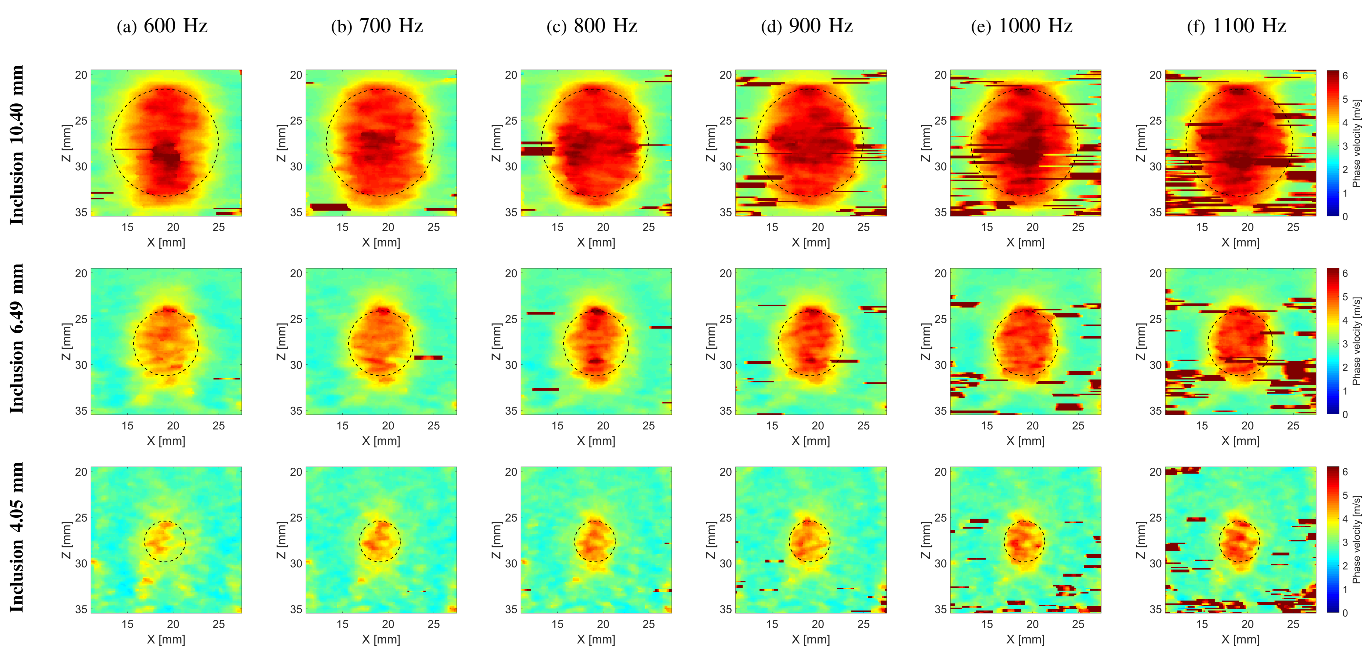

Fig. S5: Two-dimensional shear wave phase velocity images for the inclusion size of 10.40 (top row), 6.49 (middle row) and 4.05 (bottom row) diameter, respectively. Phase velocity images were calculated using phase velocity approach described by Budelli, et al. Presented images are computed for the CIRS phantom with an inclusion Type IV. Dashed lines present a true inclusion location estimated from B-modes.

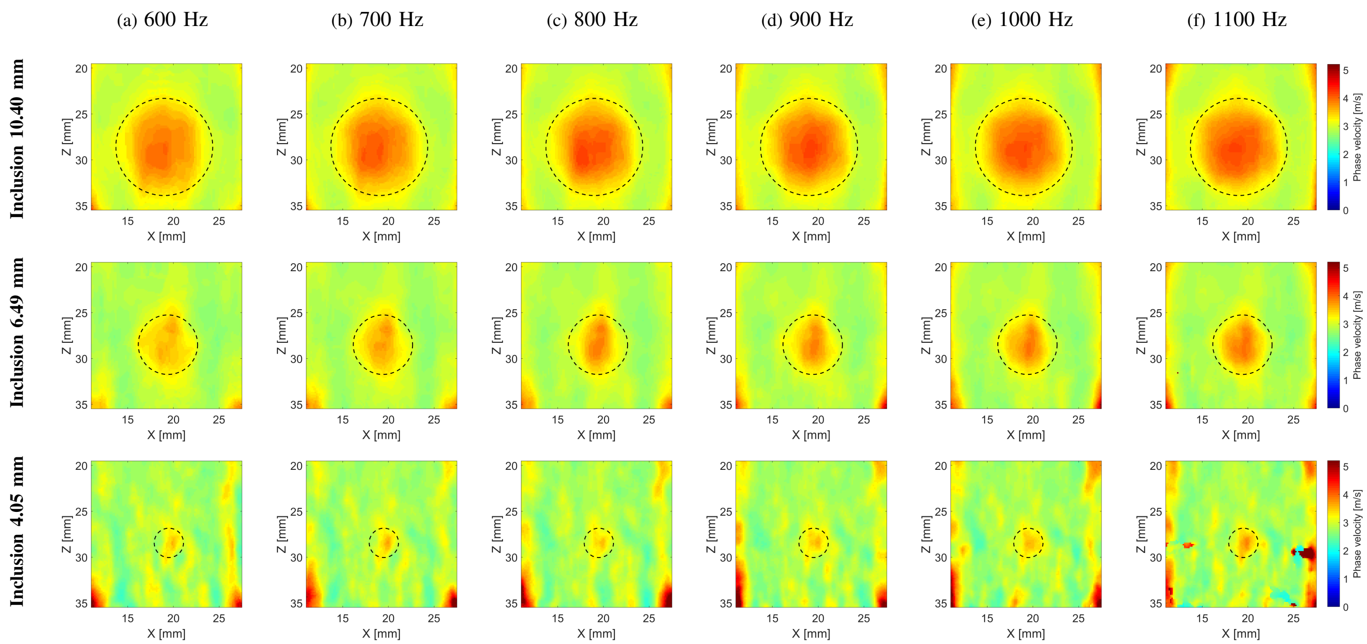

Fig. S6: Two-dimensional shear wave phase velocity images for the inclusion size of 10.40 (top row), 6.49 (middle row) and 4.05 (bottom row) diameter, respectively. Phase velocity images were calculated using LPVI approach. Presented images are computed for the CIRS phantom with an inclusion Type III. Dashed lines present a true inclusion location estimated from B-modes.

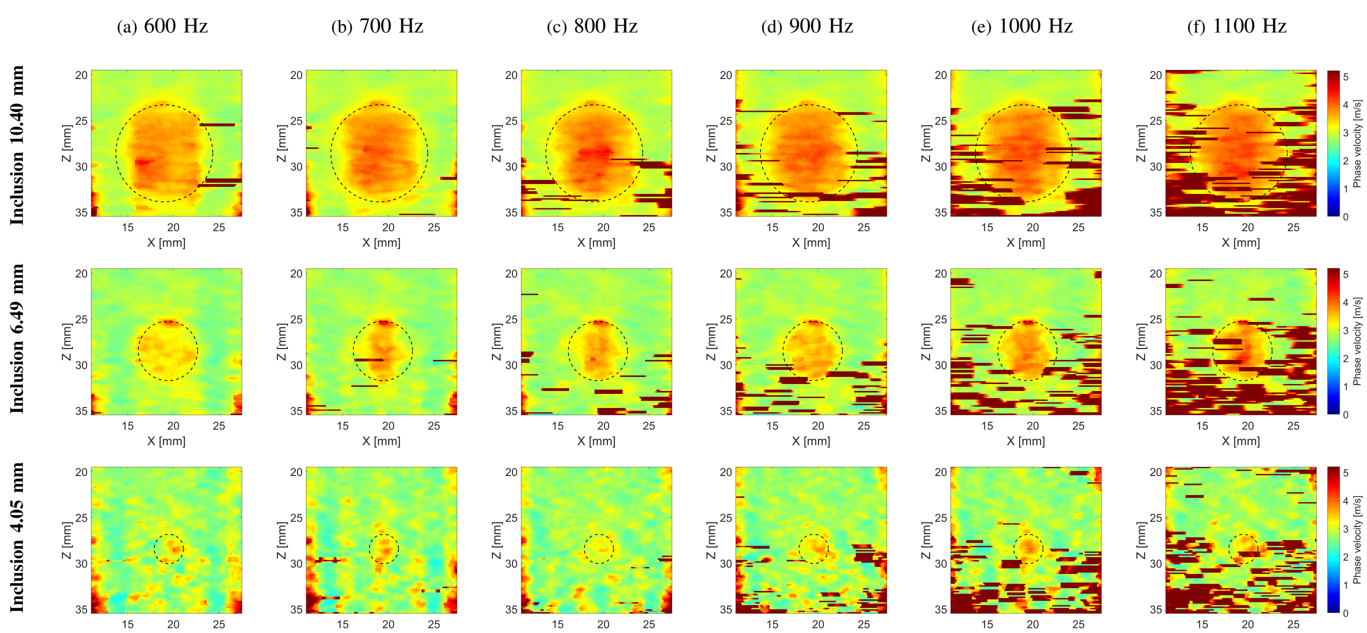

Fig. S7: Two-dimensional shear wave phase velocity images for the inclusion size of 10.40 (top row), 6.49 (middle row) and 4.05 (bottom row) diameter, respectively. Phase velocity images were calculated using phase velocity approach described by Budelli, et al. Presented images are computed for the CIRS phantom with an inclusion Type III. Dashed lines present a true inclusion location estimated from B-modes.

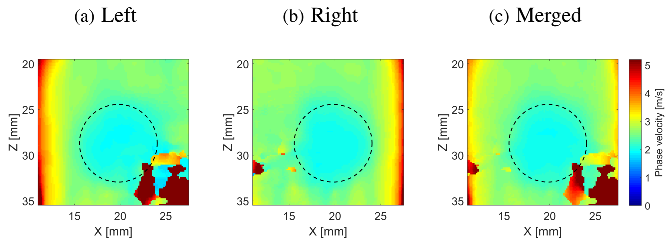

Fig. S8: Two-dimensional shear wave phase velocity images reconstructed using LPVI for the inclusion Type II and size of 10.40 mm diameter. A single frequency of 1000 Hz was applied. Reconstructions for the excitation push beam located on the (a) left and (b) right sides of the inclusion are presented. (c) presents merged image from (a) and (b). Dashed lines present a true inclusion location estimated from B-mode.

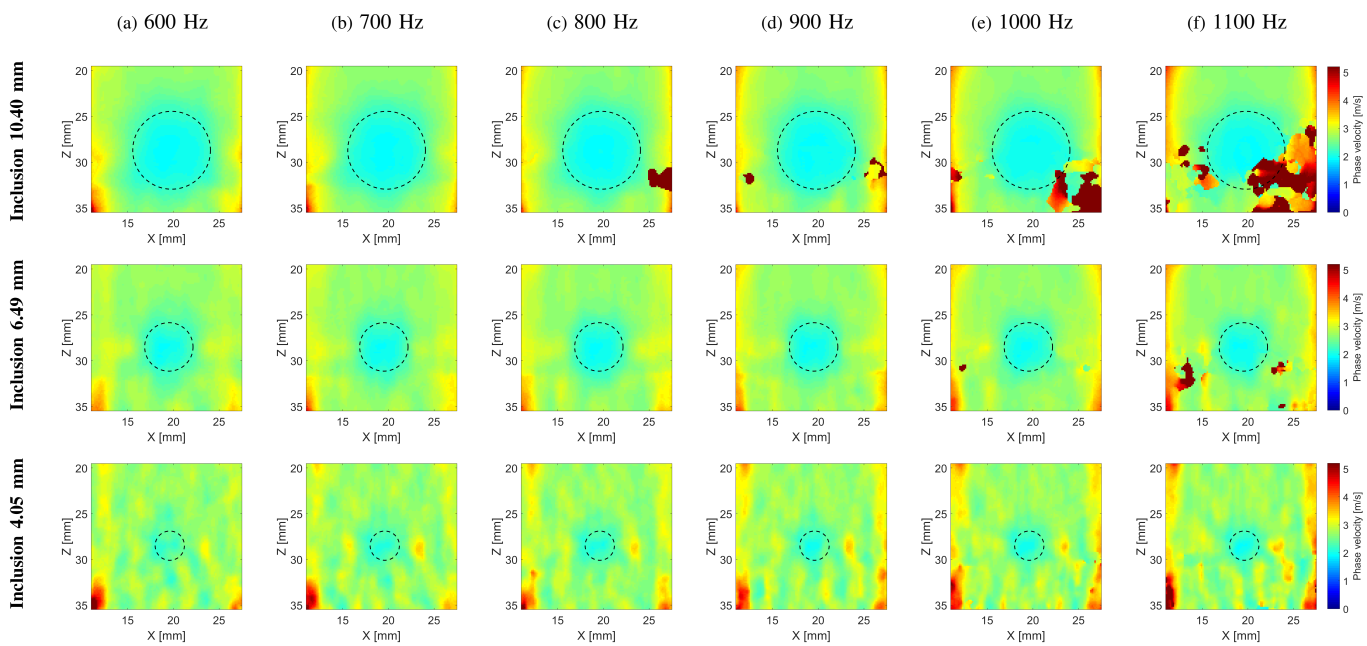

Fig. S9: Two-dimensional shear wave phase velocity images for the inclusion size of 10.40 (top row), 6.49 (middle row) and 4.05 (bottom row) diameter, respectively. Phase velocity images were calculated using LPVI approach. Presented images are computed for the CIRS phantom with an inclusion Type II. Dashed lines present a true inclusion location estimated from B-modes.

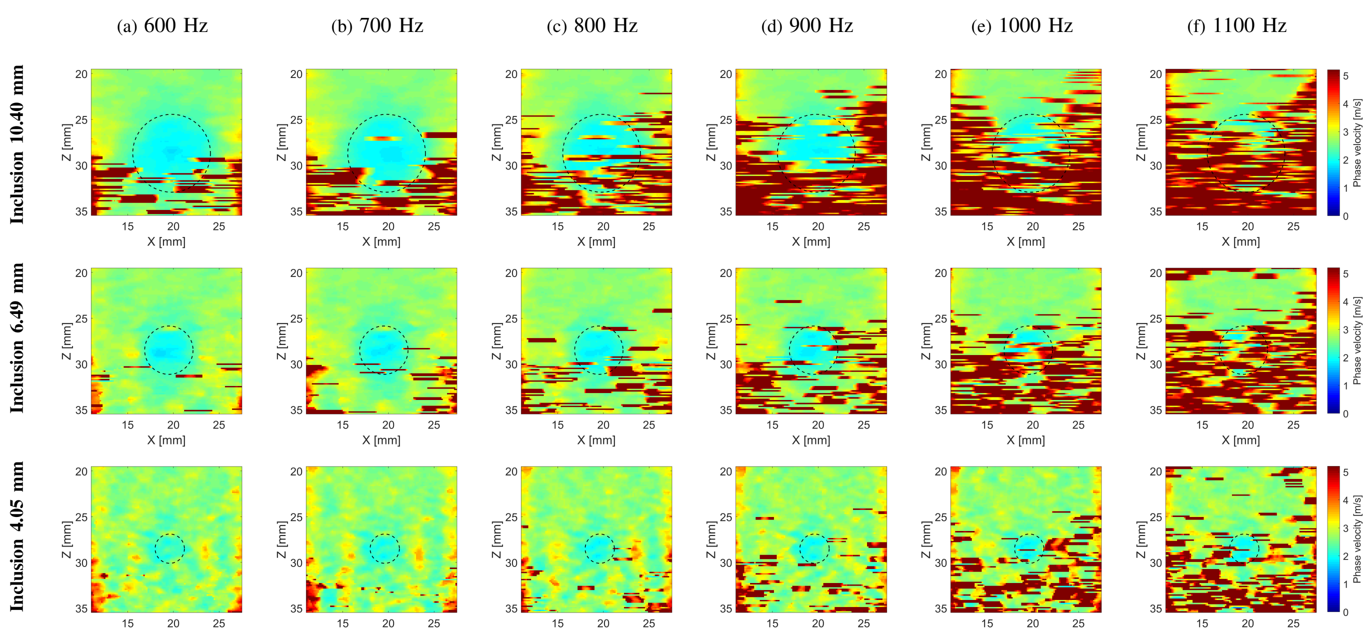

Fig. S10: Two-dimensional shear wave phase velocity images for the inclusion size of 10.40 (top row), 6.49 (middle row) and 4.05 (bottom row) diameter, respectively. Phase velocity images were calculated using phase velocity approach described by Budelli, et al. Presented images are computed for the CIRS phantom with an inclusion Type II. Dashed lines present a true inclusion location estimated from B-modes.

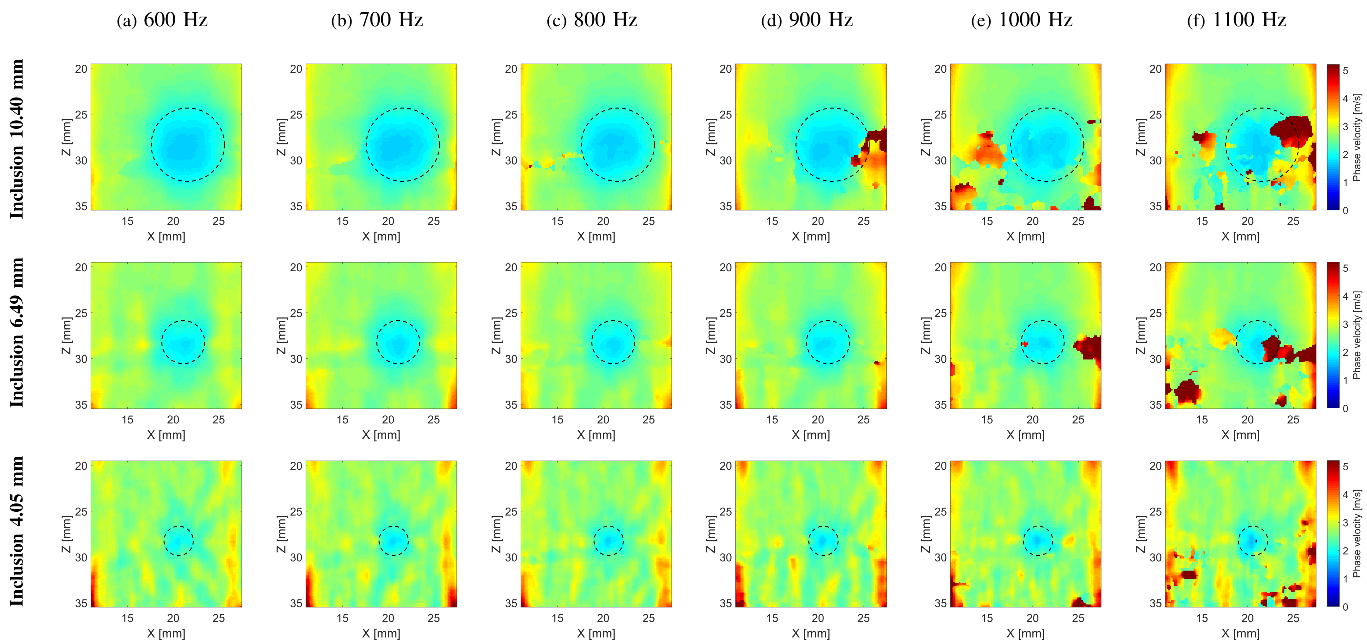

Fig. S11: Two-dimensional shear wave phase velocity images for the inclusion size of 10.40 (top row), 6.49 (middle row) and 4.05 (bottom row) diameter, respectively. Phase velocity images were calculated using LPVI approach. Presented images are computed for the CIRS phantom with an inclusion Type I. Dashed lines present a true inclusion location estimated from B-modes.

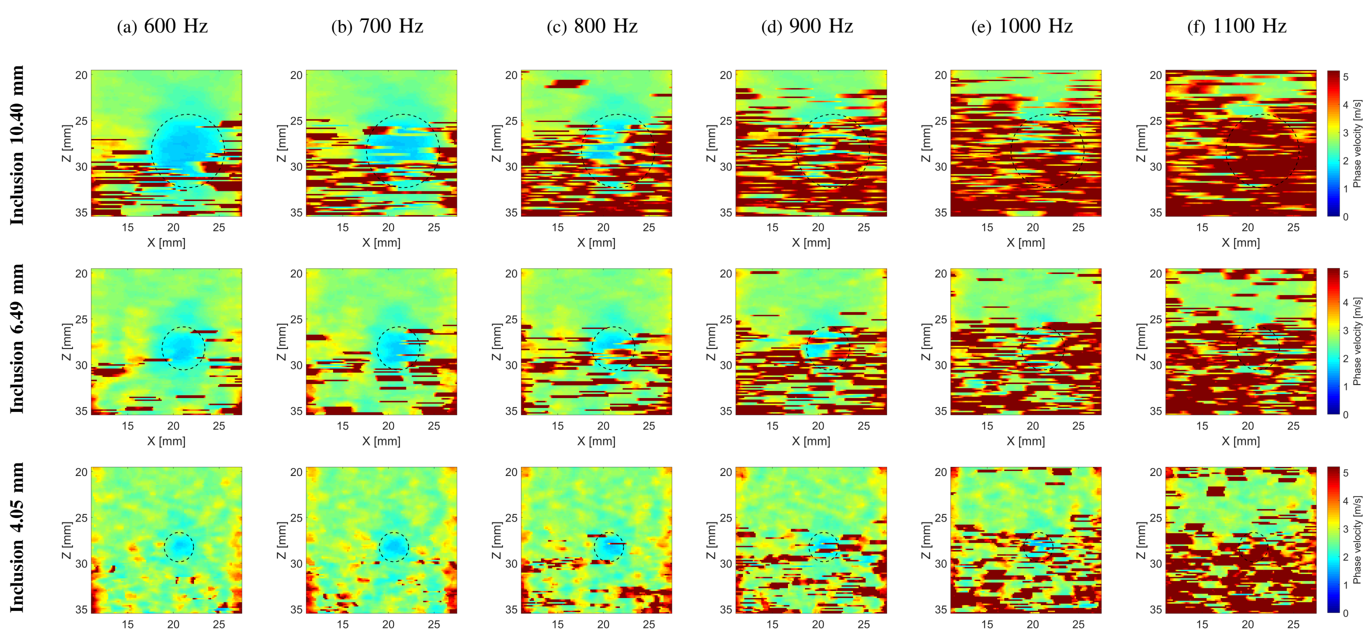

Fig. S12: Two-dimensional shear wave phase velocity images for the inclusion size of 10.40 (top row), 6.49 (middle row) and 4.05 (bottom row) diameter, respectively. Phase velocity images were calculated using phase velocity approach described by Budelli, et al. Presented images are computed for the CIRS phantom with an inclusion Type I. Dashed lines present a true inclusion location estimated from B-modes.

TABLE S4: Mean, median, standard deviation, variance, maximum and minimum values of shear wave velocity calculated for the inclusion Type IV and various sizes for LPVI approach. Values are presented in the unit of m/s. A nominal Young's modulus provided by the manufacturer is 80 kPa (c = 5.164 m/s).

Inclusion	Variable	Frequency [Hz]					
		600	**700**	**800**	**900**	**1000**	**1100**
10.40 mm	**MEAN**	4.716	4.783	4.844	4.907	4.959	4.971
	MEDIAN	4.727	4.767	4.897	5.001	5.028	5.051
	STD	0.608	0.646	0.646	0.647	0.675	0.671
	VAR	0.370	0.417	0.418	0.418	0.455	0.450
	MAX	5.958	6.143	6.132	6.030	6.151	6.119
	MIN	3.528	3.466	3.463	3.556	3.605	3.608
6.49 mm	**MEAN**	4.384	4.441	4.518	4.571	4.635	4.671
	MEDIAN	4.426	4.509	4.556	4.538	4.605	4.774
	STD	0.338	0.304	0.401	0.539	0.578	0.497
	VAR	0.114	0.092	0.161	0.290	0.334	0.247
	MAX	5.011	5.092	5.403	5.547	5.804	5.421
	MIN	3.600	3.633	3.598	3.536	3.486	3.482
4.05 mm	**MEAN**	3.898	4.044	4.187	4.249	4.271	4.362
	MEDIAN	3.838	4.022	4.201	4.281	4.237	4.356
	STD	0.391	0.291	0.282	0.337	0.361	0.356
	VAR	0.153	0.085	0.079	0.114	0.130	0.127
	MAX	4.782	4.613	4.757	4.892	5.149	5.210
	MIN	3.141	3.377	3.453	3.368	3.459	3.521

TABLE S5: Mean, median, standard deviation, variance, maximum and minimum values of shear wave velocity calculated for the inclusion Type IV and various sizes for phase velocity approach described by Budelli et al. Values are presented in the unit of m/s. A nominal Young's modulus provided by the manufacturer is 80 kPa (c = 5.164 m/s).

Inclusion	Variable	Frequency [Hz]					
		600	**700**	**800**	**900**	**1000**	**1100**
10.40 mm	**MEAN**	4.801	4.907	5.083	5.162	5.238	5.303
	MEDIAN	4.877	5.038	5.205	5.259	5.324	5.408
	STD	0.671	0.574	0.574	0.557	0.622	0.586
	VAR	0.450	0.329	0.329	0.311	0.387	0.343
	MAX	6.784	6.100	6.911	6.310	6.925	6.996
	MIN	3.283	3.226	3.316	3.493	2.907	3.525
6.49 mm	**MEAN**	4.326	4.440	4.589	4.664	4.773	4.875
	MEDIAN	4.347	4.527	4.665	4.747	4.859	4.971
	STD	0.332	0.372	0.565	0.507	0.413	0.503
	VAR	0.110	0.138	0.319	0.257	0.170	0.253
	MAX	5.344	5.546	6.460	6.775	5.712	6.989
	MIN	3.494	3.476	3.381	3.412	3.501	3.476
4.05 mm	**MEAN**	3.783	4.075	4.189	4.223	4.375	4.458
	MEDIAN	3.758	4.075	4.249	4.236	4.372	4.537
	STD	0.366	0.370	0.395	0.350	0.406	0.484
	VAR	0.134	0.137	0.156	0.122	0.165	0.234
	MAX	4.599	5.037	5.054	5.274	5.619	5.599
	MIN	3.026	3.213	3.165	3.299	3.335	3.230

TABLE S6: Mean, median, standard deviation, variance, maximum and minimum values of shear wave velocity calculated for the inclusion Type III and various sizes for LPVI approach. Values are presented in the unit of m/s. A nominal Young's modulus provided by the manufacturer is 45 kPa (c = 3.873 m/s).

Inclusion	**Variable**	**Frequency [Hz]**					
		600	**700**	**800**	**900**	**1000**	**1100**
10.40 mm	**MEAN**	3.535	3.566	3.594	3.591	3.612	3.624
	MEDIAN	3.536	3.549	3.572	3.568	3.605	3.625
	STD	0.251	0.273	0.313	0.307	0.296	0.301
	VAR	0.063	0.075	0.098	0.094	0.087	0.091
	MAX	4.054	4.100	4.203	4.223	4.183	4.148
	MIN	3.016	2.991	2.989	2.973	2.996	2.994
6.49 mm	**MEAN**	3.351	3.363	3.372	3.366	3.397	3.432
	MEDIAN	3.343	3.355	3.350	3.330	3.387	3.416
	STD	0.144	0.201	0.267	0.244	0.261	0.272
	VAR	0.021	0.040	0.071	0.060	0.068	0.074
	MAX	3.660	3.797	3.883	3.876	3.966	3.962
	MIN	2.868	2.813	2.806	2.794	2.758	2.793
4.05 mm	**MEAN**	3.132	3.178	3.195	3.241	3.283	3.323
	MEDIAN	3.198	3.208	3.221	3.244	3.290	3.332
	STD	0.238	0.226	0.158	0.152	0.157	0.243
	VAR	0.057	0.051	0.025	0.023	0.025	0.059
	MAX	3.595	3.690	3.551	3.597	3.605	3.869
	MIN	2.644	2.693	2.833	2.920	2.956	2.832

TABLE S7: Mean, median, standard deviation, variance, maximum and minimum values of shear wave velocity calculated for the inclusion Type III and various sizes for phase velocity approach described by Budelli et al. Values are presented in the unit of m/s. A nominal Young's modulus provided by the manufacturer is 45 kPa (c = 3.873 m/s).

Inclusion	**Variable**	**Frequency [Hz]**					
		600	**700**	**800**	**900**	**1000**	**1100**
10.40 mm	**MEAN**	3.552	3.586	3.660	3.692	3.766	3.933
	MEDIAN	3.588	3.624	3.637	3.703	3.741	3.820
	STD	0.274	0.284	0.361	0.379	0.439	0.617
	VAR	0.075	0.081	0.130	0.143	0.193	0.381
	MAX	6.852	4.247	6.814	6.970	6.992	6.974
	MIN	2.780	2.851	2.835	2.862	2.887	2.927
6.49 mm	**MEAN**	3.308	3.381	3.358	3.441	3.527	3.638
	MEDIAN	3.301	3.364	3.358	3.456	3.521	3.557
	STD	0.162	0.400	0.278	0.337	0.402	0.604
	VAR	0.026	0.160	0.077	0.113	0.162	0.365
	MAX	4.271	6.549	4.395	6.849	6.874	6.966
	MIN	2.832	2.682	2.689	2.793	2.715	2.739
4.05 mm	**MEAN**	3.145	3.247	3.091	3.249	3.372	3.529
	MEDIAN	3.121	3.244	3.064	3.227	3.349	3.348
	STD	0.324	0.304	0.159	0.241	0.278	0.685
	VAR	0.105	0.093	0.025	0.058	0.077	0.470
	MAX	4.064	3.994	3.611	3.939	3.984	6.796
	MIN	2.411	2.541	2.679	2.646	2.579	2.610

TABLE S8: Mean, median, standard deviation, variance, maximum and minimum values of shear wave velocity calculated for the inclusion Type II and various sizes for LPVI approach. Values are presented in the unit of m/s. A nominal Young's modulus provided by the manufacturer is 14 kPa (c = 2.160 m/s).

Inclusion	Variable	Frequency [Hz]					
		600	700	800	900	1000	1100
10.40 mm	MEAN	2.048	2.044	2.046	2.051	2.108	2.397
	MEDIAN	2.037	2.037	2.037	2.035	2.053	2.074
	STD	0.088	0.090	0.091	0.090	0.336	0.981
	VAR	0.008	0.008	0.008	0.008	0.113	0.963
	MAX	2.333	2.313	2.335	2.340	5.716	6.999
	MIN	1.900	1.897	1.908	1.915	1.933	1.904
6.49 mm	MEAN	2.116	2.102	2.077	2.093	2.102	2.099
	MEDIAN	2.120	2.096	2.077	2.096	2.100	2.095
	STD	0.101	0.102	0.093	0.094	0.099	0.105
	VAR	0.010	0.011	0.009	0.009	0.010	0.011
	MAX	2.351	2.406	2.316	2.319	2.395	2.426
	MIN	1.923	1.908	1.910	1.925	1.912	1.922
4.05 mm	MEAN	2.315	2.228	2.197	2.188	2.165	2.133
	MEDIAN	2.319	2.227	2.204	2.181	2.174	2.146
	STD	0.099	0.093	0.090	0.147	0.116	0.111
	VAR	0.010	0.009	0.008	0.022	0.014	0.012
	MAX	2.569	2.487	2.346	2.554	2.390	2.391
	MIN	2.135	2.050	2.019	1.948	1.954	1.926

TABLE S9: Mean, median, standard deviation, variance, maximum and minimum values of shear wave velocity calculated for the inclusion Type II and various sizes for phase velocity approach described by Budelli et al. Values are presented in the unit of m/s. A nominal Young's modulus provided by the manufacturer is 14 kPa (c = 2.160 m/s).

Inclusion	Variable	Frequency [Hz]					
		600	700	800	900	1000	1100
10.40 mm	MEAN	2.205	2.263	2.641	2.601	3.065	3.642
	MEDIAN	2.014	2.042	2.130	2.109	2.615	3.317
	STD	0.682	0.709	1.068	0.972	1.222	1.282
	VAR	0.466	0.503	1.142	0.944	1.493	1.645
	MAX	6.951	6.993	6.996	6.992	6.992	6.991
	MIN	1.765	1.788	1.785	1.827	1.857	1.863
6.49 mm	MEAN	2.078	2.115	2.238	2.416	3.282	3.510
	MEDIAN	2.056	2.069	2.050	2.095	2.975	3.194
	STD	0.194	0.344	0.692	0.938	1.286	1.245
	VAR	0.038	0.118	0.479	0.881	1.655	1.551
	MAX	3.062	6.179	6.123	6.994	6.932	6.980
	MIN	1.714	1.779	1.794	1.699	1.841	1.864
4.05 mm	MEAN	2.263	2.162	2.160	2.169	2.251	2.300
	MEDIAN	2.225	2.149	2.131	2.135	2.099	2.100
	STD	0.179	0.150	0.290	0.206	0.606	0.716
	VAR	0.032	0.023	0.084	0.042	0.367	0.512
	MAX	2.970	2.849	6.141	2.939	6.916	6.397
	MIN	1.986	1.846	1.839	1.840	1.792	1.808

TABLE S10: Mean, median, standard deviation, variance, maximum and minimum values of shear wave velocity calculated for the inclusion Type I and various sizes for LPVI approach. Values are presented in the unit of m/s. A nominal Young's modulus provided by the manufacturer is 8 kPa (c = 1.633 m/s).

Inclusion	Variable	Frequency [Hz]					
		600	700	800	900	1000	1100
10.40 mm	MEAN	1.848	1.865	1.887	2.061	1.923	2.361
	MEDIAN	1.832	1.844	1.872	1.867	1.890	2.014
	STD	0.126	0.146	0.145	0.747	0.182	0.975
	VAR	0.016	0.021	0.021	0.558	0.033	0.952
	MAX	2.238	2.325	2.283	6.824	3.121	6.998
	MIN	1.653	1.649	1.658	1.657	1.684	1.626
6.49 mm	MEAN	1.947	1.933	1.938	1.931	1.986	2.454
	MEDIAN	1.947	1.943	1.943	1.935	1.950	2.008
	STD	0.098	0.102	0.105	0.096	0.327	1.269
	VAR	0.010	0.010	0.011	0.009	0.107	1.610
	MAX	2.221	2.158	2.200	2.180	4.588	6.923
	MIN	1.749	1.715	1.714	1.747	1.670	1.695
4.05 mm	MEAN	2.092	2.014	2.017	2.029	2.013	2.043
	MEDIAN	2.084	2.010	2.018	2.017	2.004	1.993
	STD	0.121	0.134	0.142	0.164	0.171	0.342
	VAR	0.015	0.018	0.020	0.027	0.029	0.117
	MAX	2.412	2.443	2.346	2.514	2.486	6.460
	MIN	1.823	1.733	1.703	1.655	1.635	1.584

TABLE S11: Mean, median, standard deviation, variance, maximum and minimum values of shear wave velocity calculated for the inclusion Type I and various sizes for phase velocity approach described by Budelli et al. Values are presented in the unit of m/s. A nominal Young's modulus provided by the manufacturer is 8 kPa (c = 1.633 m/s).

Inclusion	Variable	Frequency [Hz]					
		600	700	800	900	1000	1100
10.40 mm	MEAN	2.068	2.529	3.061	3.541	3.905	4.583
	MEDIAN	1.843	2.101	2.595	3.249	3.739	4.544
	STD	0.769	1.122	1.304	1.316	1.309	1.235
	VAR	0.591	1.259	1.700	1.733	1.712	1.526
	MAX	6.964	6.996	6.999	6.990	6.986	6.998
	MIN	1.436	1.560	1.466	1.616	1.819	1.975
6.49 mm	MEAN	1.986	2.106	2.656	3.213	3.454	3.703
	MEDIAN	1.914	1.911	2.114	2.704	3.109	3.340
	STD	0.389	0.737	1.145	1.379	1.287	1.418
	VAR	0.151	0.543	1.311	1.903	1.656	2.011
	MAX	6.381	6.906	6.855	6.999	6.982	6.998
	MIN	1.614	1.629	1.641	1.669	1.628	1.741
4.05 mm	MEAN	2.081	1.978	2.068	2.404	2.922	3.857
	MEDIAN	2.036	1.963	1.971	2.117	2.394	3.638
	STD	0.241	0.223	0.567	0.948	1.312	1.438
	VAR	0.058	0.050	0.322	0.898	1.720	2.069
	MAX	2.753	2.671	6.565	6.674	6.992	6.905
	MIN	1.665	1.622	1.544	1.548	1.400	1.875

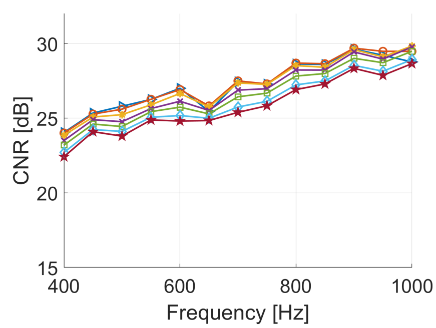

Fig. S13: The contrast-to-noise ratio (CNR) estimated for the LPVI, computed for various frequencies and the spatial window dimensions like in other plots, calculated for the gelatin phantom with the excised porcine liver inclusion.